

Rattling guest atoms in Si, Ge, and Sn-based type-II clathrate materials

Charles W. Myles^{*,1}, Jianjun Dong², and Otto F. Sankey³

¹ Department of Physics and Engineering Physics, Texas Tech University, Lubbock, TX 79409–1051, USA

² Department of Physics, Auburn University, Auburn, Alabama 36849, USA

³ Department of Physics and Astronomy, Arizona State University, Tempe, Arizona 85287, USA

Received 15 March 2003, accepted 15 April 2003

Published online 1 September 2003

PACS 63.20.Dj, 63.20.Pw, 78.30.Hv

We have studied the vibrational properties of some of the compounds based on the Type II silicon, germanium, and tin-based clathrate materials using LDA electronic structure methods. The lattices in these framework materials have open cages which can contain weakly bound guest impurities, and these guests produce local (“rattling”) vibrational modes. Such modes may scatter the extended, heat carrying acoustic vibrational modes of the framework, potentially reducing the thermal conductivity. We present results for the vibrational spectra of the Type II clathrate compounds $\text{Na}_{16}\text{Cs}_8\text{Si}_{136}$, $\text{Na}_{16}\text{Cs}_8\text{Ge}_{136}$, and $\text{Cs}_{24}\text{Sn}_{136}$. We discuss trends in the vibrational spectra of the framework host material and of the localized, rattling frequencies of the guest modes as the host changes from Si to Ge to Sn.

© 2003 WILEY-VCH Verlag GmbH & Co. KGaA, Weinheim

1 Introduction

In addition to their ground state, tetrahedrally coordinated, sp^3 -bonded, diamond lattice structure, the Group IV elements Si, Ge, and Sn can also form zeolite-like, expanded volume phases called the clathrates. These are open-framework structures in which the lattice contains large (20-, 24-, and 28-atom) cages, and in which all framework atoms are in a four-fold-coordinated sp^3 bonding configuration. The local bonding in the framework of the clathrate lattices is thus similar to that in the diamond structure. However these lattices contain pentagonal rings, which makes their topology quite different from that in the diamond lattice. Further, the “cages” formed by the Group IV atoms can house “guest” atoms, and the choice of guest may be used to tune the properties of the material, including the vibrational properties. Most of the clathrates which have been realized in the laboratory have been guest-containing compounds.

These Group IV atom-based clathrate materials continue to be of considerable interest due to their unique transport properties. In particular, they have potential thermoelectric [1–4], superconducting [5–8] and electro-optic applications [9, 10]. Among the interesting properties the clathrate compounds possess is their low thermal conductivity. The origin of this is the weak bonding of the guest atoms residing inside the cages. This results in localized (“rattler”) vibrational modes which couple to the lattice modes by resonantly scattering the acoustic-mode, heat-carrying phonons of the host framework material [1], thereby lowering the thermal conductivity.

Of the two clathrate lattice types, Group IV compounds with the Type I clathrate crystal structure have been the more thoroughly investigated both experimentally and theoretically. The pure framework materials of this type have a simple cubic lattice structure with 46 atoms per unit cell and are denoted as

* Corresponding author: e-mail: Charley.Myles@ttu.edu. Phone: (806) 742-3768. Fax: (806) 742-1182.

X_{46} ($X = \text{Si, Ge, or Sn}$). Several experimental studies of compounds based on these Type I materials (with various guest atoms in the cages) have been carried out, including transport and optical studies. The low thermal conductivity measured in these compounds is due to the weak guest-host electronic interactions, which leads to strong coupling between the localized guest rattler vibrations and the host acoustic modes. This interpretation is consistent with transport [11–18], Raman scattering [19] and acoustic measurements [20, 21] as well as with theoretical calculations [22, 23]. Several theoretical studies of the electronic, structural, and vibrational properties of both the pure Type I clathrate materials and various compounds based on the Type I lattice structure have also been carried out [24–33]. A recent theoretical-experimental study [25] of $\text{Cs}_8\text{Ga}_8\text{Sn}_{38}$ found excellent agreement between Raman scattering measurements and density functional-based calculations of the host vibrational modes and of the localized rattler modes due to the Cs guests.

In contrast to the Type I clathrates, there have been only a few experimental and theoretical studies of the Type II clathrate materials. The pure type-II materials are denoted as X_{136} ($X = \text{Si, Ge, or Sn}$). The vibrational modes of the Type II “empty” framework clathrates Si_{136} [29, 34, 35], Ge_{136} [26] and Sn_{136} [25] have been theoretically investigated due to their interest for thermoelectric and superconducting applications. Raman scattering spectra of $\text{Na}_x\text{Si}_{136}$ have also been reported [36]. Recently, structural properties have been reported for stoichiometric Si and Ge clathrates, i.e. with all the crystallographic sites within the polyhedra of the Type II structure occupied [37–39]. Transport [39] and NMR experiments have shown that the stoichiometric compounds $\text{Na}_{16}\text{Cs}_8\text{Si}_{136}$ and $\text{Na}_{16}\text{Cs}_8\text{Ge}_{136}$ are metallic. There have also been temperature-dependent X-ray diffraction measurements of the low lying vibrational modes of the Cs atoms inside the cages of these Type II Si and Ge based clathrates [39].

In this paper, we report the results of a density functional-based theoretical study of the vibrational modes of the Type II clathrate compounds $\text{Na}_{16}\text{Cs}_8\text{Si}_{136}$, $\text{Na}_{16}\text{Cs}_8\text{Ge}_{136}$, and $\text{Cs}_{24}\text{Sn}_{136}$. We compute the phonon dispersion relations, $\omega(q)$, for these materials and identify the localized mode, “rattling” branches induced by the guests. Because of their potential importance in lowering the thermal conductivity in these materials, in this study, we focus on the low-lying rattling modes of the Na and Cs guests in the large 28-atom and small 20-atom cages (described below). This work is a follow up to a recently published Raman scattering study [40] by us and others of the Type II materials Si_{136} , $\text{Na}_{16}\text{Cs}_8\text{Si}_{136}$ and $\text{Na}_{16}\text{Cs}_8\text{Ge}_{136}$. In that study, the vibrational frequencies near $q = 0$ in these materials were determined experimentally and compared with density functional-based calculations. It was found that the measured vibrational modes of both the host framework and the guests are in excellent agreement with the calculations. By including $\text{Cs}_{24}\text{Sn}_{136}$ in the present paper, we extend the work of Ref. [40] to the Sn-based clathrates and we also extend the work of Ref. [25] on the vibrational properties of Sn-based clathrates to Type II Sn-clathrate compounds. Including $\text{Cs}_{24}\text{Sn}_{136}$ in this study also allows us to seek trends in vibrational frequencies of Cs guests in the large cages as the host framework changes from Si to Ge to Sn. The compounds $\text{Na}_{16}\text{Cs}_8\text{Si}_{136}$ and $\text{Na}_{16}\text{Cs}_8\text{Ge}_{136}$ have been synthesized and characterized in the laboratory [40]. Currently $\text{Cs}_{24}\text{Sn}_{136}$ remains a hypothetical material.

2 Computational details

The pure Type II clathrate framework X_{136} ($X = \text{Si, Ge, or Sn}$) is a face centered cubic structure with 136 atoms per cubic unit cell. All of the compounds considered here have the same symmetry as their “parent” framework lattice. For $\text{Na}_{16}\text{Cs}_8\text{Si}_{136}$ and $\text{Na}_{16}\text{Cs}_8\text{Ge}_{136}$, each of the 20-atom cages is occupied by guest Na’s and each of the (larger) 28-atom cages is occupied by guest Cs’s. In $\text{Cs}_{24}\text{Sn}_{136}$, all of the large and small cages are occupied by Cs’s. Further details of the crystalline structures of these materials may be found in Refs. [25, 26, 31, 40].

Our calculations are based on the local density approximation (LDA) to density functional theory and they use a planewave basis with ultrasoft pseudopotentials [41, 42]. The Vienna Ab-initio Simulation Package (VASP) [43, 44] has been used with the Ceperley–Alder functional [45] to approximate the exchange-correlation energy. This method has been extensively tested on a wide variety of systems. The implementation we use is particularly efficient for the large clathrate unit cells. This technique has been

adopted in our previous studies of Si [29, 46] and Ge [26, 30] and Sn [24, 25] clathrates. In those studies, the calculated structural and vibrational properties were found to be in good agreement with experimental data [47–50]. The effects of the generalized gradient approximation (GGA) correction to the LDA were examined in Ref. [29] and were found to be minor. Thus, we neglect these corrections here.

The procedures we have used to compute the lattice vibrational dispersion relations for the materials of interest here are the same as those we have used in earlier LDA studies of the vibrational properties of the clathrates [25, 26, 29]. The reader is referred to previous work for details and only a very brief description will be given here. Beginning with assumed interatomic distances and bond angles, the first step is to optimize the structure by minimizing the total electronic binding energy. This is accomplished by relaxing the internal coordinates at a given volume. This is repeated for several volumes until an LDA minimum energy configuration (internal and external coordinates) is obtained. Once the equilibrium lattice geometry is obtained by this method, all ground state properties of the material can be obtained, including electronic bandstructures and vibrational dispersion relations. We have computed the bandstructures of $\text{Na}_{16}\text{Cs}_8\text{Si}_{136}$, $\text{Na}_{16}\text{Cs}_8\text{Ge}_{136}$, and $\text{Cs}_{24}\text{Sn}_{136}$. As expected from the extra valence electrons introduced by the Na and Cs guests, we find that each material is metallic. Since our focus here is vibrational properties, we do not display the energy bands here.

Starting with the LDA-optimized equilibrium (zero force) structure which results from the procedure just described, we next obtain the dynamical matrix, $D(q)$. Within the harmonic approximation, diagonalization of $D(q)$ gives the vibrational mode eigenvalues and eigenvectors. A calculation of $D(q)$ in principle requires the computation of second derivatives of the LDA-binding energy with respect to atomic displacements. In our approach to this problem [25, 26, 29], small, finite atomic displacements U_0 are used to compute forces within the LDA. Within the harmonic approximation, these forces are proportional to the displacements. Dividing these forces by the displacements U_0 gives the matrix elements of $D(q)$. Also, we calculate $D(q)$ with both $+U_0$ and $-U_0$ and average the two matrices. Any odd-order anharmonicity then vanishes, leaving only fourth or higher (even) order anharmonic errors.

Group theory is used to greatly reduce the number and symmetries of the displacements U_0 that need to be considered. Our procedure assumes that the harmonic approximation is valid. Since our method relies on finite displacements, this assumption must be carefully checked. With the exception of the rattler modes associated with the Cs guests in the large cages in $\text{Cs}_{24}\text{Sn}_{136}$, we have found the harmonic approximation to be valid for all of the vibrational modes in the materials considered here. For these harmonic modes we have used $U_0 = 0.02 \text{ \AA}$. We have found the modes produced by the Cs motion in the 28-atom cages in $\text{Cs}_{24}\text{Sn}_{136}$ to be *very* anharmonic. These anharmonic Cs guest modes are discussed further in the next section. Once $D(q)$ is determined, as outlined in detail elsewhere [25, 26, 29], it is diagonalized to obtain the vibrational eigenvalues and eigenvectors.

3 Results

3.1 Dispersion relations for $\text{Na}_{16}\text{Cs}_8\text{Si}_{136}$, $\text{Na}_{16}\text{Cs}_8\text{Ge}_{136}$, and $\text{Cs}_{24}\text{Sn}_{136}$

The calculated vibrational dispersion curves for $\text{Na}_{16}\text{Cs}_8\text{Si}_{136}$, $\text{Na}_{16}\text{Cs}_8\text{Ge}_{136}$, and $\text{Cs}_{24}\text{Sn}_{136}$, are shown in Figs. 1–3. Each of these figures is qualitatively similar and shares the common features that the small Brillouin zone coming from the large unit cells causes narrow bands, that most of the optical modes are very flat, as is reminiscent of “zone folding”, and that there are two major, high density of states regions in the spectrum. The flat optical modes of course result in very small group velocities $[d\omega(q)/dq]$. According to semi-classical heat transport theory [51], phonons with small velocities transfer heat inefficiently. This suggests that these materials should have low thermal conductivities. Both experimental measurements [12–14] and calculations of the thermal conductivity of the Type I clathrates [23] have shown that this suggestion has validity. As is to be expected, as the host framework is changed from Si to Ge to Sn, the heavier mass of the host atom causes the maximum vibrational energy to decrease, with the spectrum and all of the mentioned features compressed into a smaller energy region.

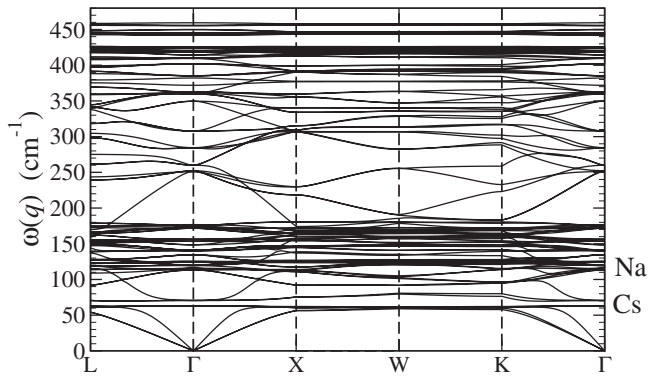


Fig. 1 Phonon dispersion relations for $\text{Na}_{16}\text{Cs}_8\text{Si}_{136}$.

3.1.1 $\text{Na}_{16}\text{Cs}_8\text{Si}_{136}$

The dispersion curves for $\text{Na}_{16}\text{Cs}_8\text{Si}_{136}$ are shown in Fig. 1. Similar results for the “parent” framework material Si_{136} were obtained in Ref. [29]. The acoustic modes are located below about 50 cm^{-1} and the optic modes are located from about 80 cm^{-1} to about 490 cm^{-1} . The optic modes are approximately separated into three bands. There is a low frequency, high density of states band from about 100 cm^{-1} to up to about 175 cm^{-1} , a medium frequency, high density of states band from about 200 cm^{-1} to up to about 450 cm^{-1} , and a narrow, high frequency band from about 450 cm^{-1} to up to about 490 cm^{-1} . The weak bonding of the Na and Cs guests in the small and large cages, respectively, leads to localized, relatively low frequency rattler modes associated with these atoms. An eigenvector analysis shows that the Na motion in the small (20-atom) cages, leads to localized modes in a narrow region around 118 cm^{-1} to 121 cm^{-1} . These modes are labelled by “Na” on the right side of Fig. 1. Similarly, we find that the Cs motion in the large (28 atom) cages leads to local vibrational modes at about 65 cm^{-1} to 67 cm^{-1} . In Fig. 1, these modes are labelled by “Cs” on the right side. A model for the Cs guest modes is discussed in Sect. 3.2.

In Ref. [29], it was found that the acoustic modes of the framework material Si_{136} were located below about 80 cm^{-1} . We note that the very flat Cs guest rattler modes in $\text{Na}_{16}\text{Cs}_8\text{Si}_{136}$ occur in the middle of the host Si_{136} acoustic mode region. As expected, the presence of the heavy Cs atoms in the large cages in $\text{Na}_{16}\text{Cs}_8\text{Si}_{136}$ has thus compressed the host acoustic mode bandwidth. Further, according to heat transport theory [51], the resulting, almost dispersionless Cs rattler modes in that region can efficiently scatter with the heat-carrying host acoustic modes, potentially suppressing the thermal conductivity. We have also examined the frequencies and symmetries of the $q = 0$ vibrational modes in $\text{Na}_{16}\text{Cs}_8\text{Si}_{136}$ and have determined the Raman-active modes. Further, we have found excellent agreement between our predictions for these modes and Raman scattering experiments. These results are presented elsewhere [40].

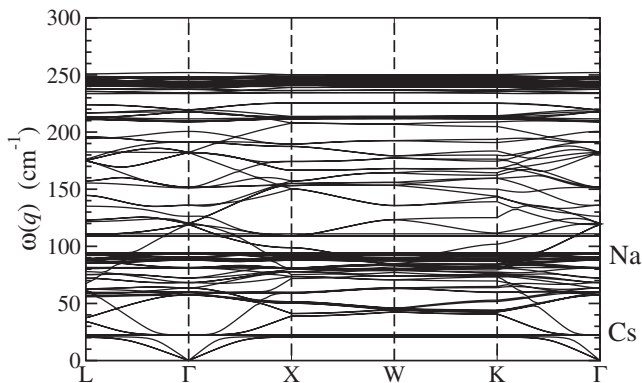


Fig. 2 Phonon dispersion relations for $\text{Na}_{16}\text{Cs}_8\text{Ge}_{136}$.

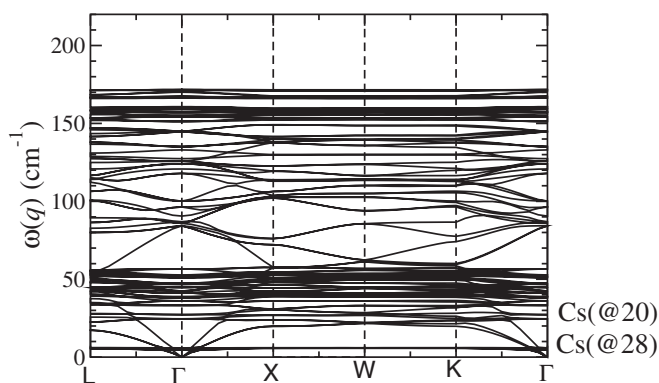


Fig. 3 Phonon dispersion relations for $\text{Cs}_{24}\text{Sn}_{136}$.

3.1.2 $\text{Na}_{16}\text{Cs}_8\text{Ge}_{136}$

The dispersion curves for $\text{Na}_{16}\text{Cs}_8\text{Ge}_{136}$ are shown in Fig. 2 and are qualitatively similar to those just discussed for $\text{Na}_{16}\text{Cs}_8\text{Si}_{136}$. As expected from the heavier mass of the Ge host atoms compared with that for Si, all of the features of the $\text{Na}_{16}\text{Cs}_8\text{Ge}_{136}$ spectrum are compressed into a smaller energy range than that for $\text{Na}_{16}\text{Cs}_8\text{Si}_{136}$. The dispersion curves for Ge_{136} , the “parent” framework material for $\text{Na}_{16}\text{Cs}_8\text{Ge}_{136}$, may be found in Ref. [26]. The acoustic mode region for $\text{Na}_{16}\text{Cs}_8\text{Ge}_{136}$ is below about 25 cm^{-1} and the optic mode region is from about 40 cm^{-1} to about 255 cm^{-1} . There are again approximately three optic bands. A low frequency, high density of states band occurs from about 60 cm^{-1} to up to about 95 cm^{-1} , a medium frequency band occurs from about 110 cm^{-1} to up to about 230 cm^{-1} , and a very narrow, high frequency, high density of states band occurs from about 230 cm^{-1} to up to about 255 cm^{-1} . The loosely bound Na and Cs guests in the small and large cages again lead to localized, low frequency rattler modes associated with these atoms. An eigenvector analysis shows that the Na motion in the 20-atom cages leads to localized modes in a narrow region around 89 cm^{-1} to 94 cm^{-1} . Similarly, the Cs motion in the 28 atom cages leads to local vibrational modes at about 21 cm^{-1} to 23 cm^{-1} . These rattler modes are labelled on the right of Fig. 2 by “Na” and “Cs” at the appropriate frequency. As expected, because of the larger cage and the heavier mass of the Ge host atoms, these rattler modes have moved down in frequency in comparison to those found in $\text{Na}_{16}\text{Cs}_8\text{Si}_{136}$. A model for the Cs rattler modes and for the trends in these modes as the host framework changes is discussed in Sect. 3.2.

The acoustic modes of the framework material Ge_{136} found in Ref. [26] were confined to below about 50 cm^{-1} . Similar to the case for $\text{Na}_{16}\text{Cs}_8\text{Si}_{136}$, the Cs guest rattler modes in $\text{Na}_{16}\text{Cs}_8\text{Ge}_{136}$ occur in the middle of the host Ge_{136} acoustic mode region, so that as expected, the heavy Cs atom motion in the large cages has compressed the host acoustic mode bandwidth. According to heat transport theory [51], these very flat Cs rattler modes can efficiently scatter with the host acoustic modes and can thus potentially suppress the thermal conductivity. We have also computed the frequencies and symmetries of the $q = 0$ vibrational modes in $\text{Na}_{16}\text{Cs}_8\text{Ge}_{136}$ and have obtained the Raman-active modes. The results presented in Ref. [40] show that there is excellent agreement between our predicted modes and Raman scattering experiments.

3.1.3 $\text{Cs}_{24}\text{Sn}_{136}$

The compound $\text{Cs}_{24}\text{Sn}_{136}$ is qualitatively different than the others considered here because the heavier Cs guest atoms occupy both the small (20 atom) and the large (28 atom) cages. The dispersion curves for this material are shown in Fig. 3. Again, as expected from the heavier mass of the Sn host atoms compared with Ge, all of the features of the $\text{Cs}_{24}\text{Sn}_{136}$ spectrum are compressed into a smaller energy range than that for $\text{Na}_{16}\text{Cs}_8\text{Ge}_{136}$. The dispersion curves for Sn_{136} , the “parent” framework material for $\text{Cs}_{24}\text{Sn}_{136}$, may be found in Ref. [25]. The acoustic mode region for $\text{Cs}_{24}\text{Sn}_{136}$ is below about 18 cm^{-1} and the optic mode region is from about 25 cm^{-1} to about 170 cm^{-1} . As in the other materials, there are ap-

proximately three optic bands. A low frequency, high density of states band occurs from about 40 cm^{-1} to up to about 55 cm^{-1} , a medium frequency band occurs from about 80 cm^{-1} to up to about 140 cm^{-1} , and a narrow, high frequency, high density of states band occurs from about 150 cm^{-1} to up to about 170 cm^{-1} . The loosely bound Cs guests in the small and large cages again lead to localized, low frequency rattler modes associated with these atoms. An eigenvector analysis shows that the Cs motion in the 20-atom cages leads to localized modes in a narrow region around 25 cm^{-1} to 30 cm^{-1} . These modes are labelled with “Cs(@20)” to the right of Fig. 3. Further, the Cs motion in the 28 atom cages leads to local vibrational modes at *extremely* small frequencies from 5 cm^{-1} to 7 cm^{-1} , which are labelled on the right of Fig. 3 with “Cs(@28)”. As expected, because of the larger cage and the heavier mass of the Sn host atoms, these rattler modes have moved down considerably in frequency in comparison to those found in $\text{Na}_{16}\text{Cs}_8\text{Ge}_{136}$. Predictions of such low frequencies demand that our results be interpreted with caution. We discuss this next.

In our calculations of the dispersion relations for $\text{Cs}_{24}\text{Sn}_{136}$, we have found that the low-lying (rattling) vibrational modes of the Cs guests in the large (28 atom) cages are sensitive to the choice of the finite displacement U_0 used in the calculation of the dynamical matrix $D(q)$. For these modes *only*, it was necessary to use the relatively large displacement of $U_0 = 0.07\text{ \AA}$ in order to obtain a physically realistic phonon spectrum. This should be compared with the value of $U_0 = 0.02\text{ \AA}$ which we have used to calculate all of the other vibrational modes presented in this paper. For these Cs rattling modes *only*, using $U_0 = 0.02\text{ \AA}$ resulted in some imaginary frequencies. This is not a sign of a dynamic instability, but is an artifact which is due to the extremely weak bonding of Cs in the large cages, which causes the modes associated with it to be *extremely* anharmonic. To test the sensitivity of these rattling modes to the choice of U_0 , we have also computed them using $U_0 = 0.08\text{ \AA}$. We find that the predicted frequencies change by less than 2% when U_0 is increased in this way. The sensitivity of these rattling modes to the choice of U_0 is likely an intrinsic limitation of the application of the harmonic approximation to the very weakly bound Cs guests in the large cages in $\text{Cs}_{24}\text{Sn}_{136}$. Our predicted Cs rattler mode frequencies of 5 cm^{-1} to 7 cm^{-1} should thus be interpreted with this sensitivity to U_0 in mind. The weakly bound Cs guests in the 28 atom cages in this material are further discussed in Sect. 3.2 in the context of a model for the trends in the Cs rattler modes as the host changes from Si to Ge to Sn.

3.2 Model for Trends in Guest Rattler Frequencies

The trends in the localized guest rattler frequencies of Cs in the large (28-atom) cages in $\text{Na}_{16}\text{Cs}_8\text{Si}_{136}$, $\text{Na}_{16}\text{Cs}_8\text{Ge}_{136}$, and $\text{Cs}_{24}\text{Sn}_{136}$ as the host is changed from Si to Ge to Sn are very interesting and therefore warrant further discussion. To place this discussion on a quantitative basis, we have developed a simple model to help to explain the trends in these Cs rattling modes. Using as input some of the results for the LDA-optimized lattice structures for the three materials, this model examines the large size of the cage, compared to the size of the host and guest atoms, and correlates it with the restoring force on the rattling guest Cs atom.

The LDA calculated, nearest-neighbor Si–Si, Ge–Ge, and Sn–Sn distances in $\text{Na}_{16}\text{Cs}_8\text{Si}_{136}$, $\text{Na}_{16}\text{Cs}_8\text{Ge}_{136}$, and $\text{Cs}_{24}\text{Sn}_{136}$ are in the ranges $2.32\text{--}2.38\text{ \AA}$, $2.44\text{--}2.48\text{ \AA}$, and $2.83\text{--}2.91\text{ \AA}$ respectively. These results give an estimate of the covalent radii of the framework atoms of $r_{\text{Si}} = 1.18\text{ \AA}$, $r_{\text{Ge}} = 1.23\text{ \AA}$, and $r_{\text{Sn}} = 1.44\text{ \AA}$, which are in line with conventional estimates [52]. From the LDA-optimized structures, we obtain the Cs guest-to-framework atom distance, which gives a estimate of the size of the large cages. For the Si-, Ge- and Sn-based materials these distances are in the ranges $3.88\text{--}3.97\text{ \AA}$ (Cs–Si), $4.10\text{--}4.18\text{ \AA}$ (Cs–Ge), and $4.67\text{--}4.83\text{ \AA}$ (Cs–Sn). From these results, estimates of the average radius, r_{cage} , of the 28-atom cages in the three materials can be obtained. These are $r_{\text{cage}}(\text{Cs–Si}) = 3.93\text{ \AA}$, $r_{\text{cage}}(\text{Cs–Ge}) = 4.14\text{ \AA}$, and $r_{\text{cage}}(\text{Cs–Sn}) = 4.75\text{ \AA}$. A simple estimate of the size of Cs is its ionic radius, $r_{\text{Cs}} = 1.69\text{ \AA}$ [52]. From these values, one can obtain a measure of how tight-fitting a Cs atom is inside its cage. We define an “excess” radius Δr as $\Delta r \equiv r_{\text{cage}} - (r_{\text{X}} + r_{\text{Cs}})$, where r_{X} is the estimated covalent radius of the framework atom (X=Si, Ge, or Sn). Clearly, Δr is a measure of how loosely fitting a Cs guest atom is inside its 28 host atom cage.

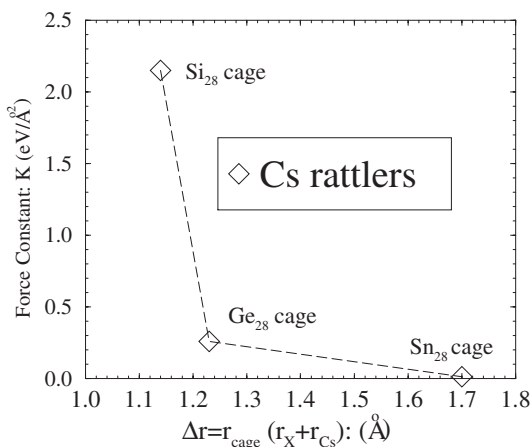


Fig. 4 Effective force constant K as a function of $r = r_{\text{cage}} - (r_X + r_{\text{Cs}})$, obtained from the model described in the text. Here $X = \text{Si, Ge, and Sn}$.

For $\text{Na}_{16}\text{Cs}_8\text{Si}_{136}$, $\text{Na}_{16}\text{Cs}_8\text{Ge}_{136}$, and $\text{Cs}_{24}\text{Sn}_{136}$, the excess radii are $\Delta r = 1.06 \text{ \AA}$, 1.22 \AA , and 1.62 \AA , respectively. Clearly, the cages are all “over-sized”. It is worth remarking that the Cs guests in the 28-atom cages in $\text{Cs}_{24}\text{Sn}_{136}$ correspond to the largest alkali metal atom, Cs, inside the largest cages, Sn_{28} , of any of the Group IV clathrate materials. Nevertheless, the Sn_{28} cages are clearly exceptionally “over-sized” in comparison with the Cs guest. For a more conservative estimate of the cage size in comparison with guest atom size, one might use the atomic radius of Cs (2.65 \AA) [52] instead of the ionic radius. This gives only slightly oversized cages for $\text{Na}_{16}\text{Cs}_8\text{Si}_{136}$ and $\text{Na}_{16}\text{Cs}_8\text{Ge}_{136}$ ($\Delta r = 0.10 \text{ \AA}$ and 0.26 \AA , respectively). However, for $\text{Cs}_{24}\text{Sn}_{136}$, it still produces a large over-sized cage with $\Delta r = 0.66 \text{ \AA}$. In the model discussed below, we use the Cs ionic radius. These rough size arguments are clearly consistent with the very weak binding, the resulting very low vibrational frequencies, and the extreme anharmonicity of the potential that we have found for the Cs’s in the Sn_{28} cages.

Correlating these size estimates with the LDA results for the rattler frequencies of the Cs guest atoms in the large cages shows that the cage size in the three materials significantly influences the rattler frequencies. To help to explain the trend that the Cs rattler frequencies decrease as the host changes from Si to Ge to Sn, we use a simple harmonic oscillator model in which the effective spring constant for these modes is determined by assuming that the motion is just that of Cs. In this crude picture, the rattler mode frequency ω_R is given by $\omega_R = (K/M)^{1/2}$ where M is the atomic mass of Cs (132.9 au) and K is an effective force constant for the rattler mode. Thus K , which we fit to the LDA-calculated rattler frequency results, is a measure of the strength (or weakness) of the guest-host interaction.

Figure 4 shows the resulting effective force constant K for Cs in the Si_{28} , Ge_{28} , and Sn_{28} cages in $\text{Na}_{16}\text{Cs}_8\text{Si}_{136}$, $\text{Na}_{16}\text{Cs}_8\text{Ge}_{136}$, and $\text{Cs}_{24}\text{Sn}_{136}$. Even in the smallest Si_{28} cage, the effective spring constant is less than $2.2 \text{ eV}/(\text{\AA})^2$. This should be compared with a similarly computed K for Si–Si bonds in the Si clathrates [22], which is of order $10 \text{ eV}/(\text{\AA})^2$. This clearly shows that Cs in $\text{Na}_{16}\text{Cs}_8\text{Si}_{136}$ is weakly bound, consistent with the calculated frequencies and with the above discussion. As is seen in Fig. 4, the effective K for Cs rattlers in the Ge_{28} cages in $\text{Na}_{16}\text{Cs}_8\text{Ge}_{136}$ is dramatically reduced by nearly one order of magnitude from that in $\text{Na}_{16}\text{Cs}_8\text{Si}_{136}$. It should be noted that this large reduction in K occurs even though the Δr for the Ge_{28} cage is only about 0.16 \AA larger than that for the Si_{28} cage. Since the effective K for Ge–Ge bonds in the Ge clathrates [26] is also of the order of $10 \text{ eV}/(\text{\AA})^2$, this shows that Cs rattlers in $\text{Na}_{16}\text{Cs}_8\text{Ge}_{136}$ are even more weakly bound than they are in $\text{Na}_{16}\text{Cs}_8\text{Si}_{136}$. Finally, Cs’s in the oversized Sn_{28} cages in $\text{Cs}_{24}\text{Sn}_{136}$, which produce extremely low rattler frequencies, give an effective force constant K which is nearly zero (in contrast to the effective K for Sn–Sn bonds of $\sim 8 \text{ eV}/(\text{\AA})^2$ [25]). This is consistent with the above conclusion that the Cs guests are barely bound in this material.

4 Conclusions

We have performed an LDA-based study of the lattice vibrational spectra of the Type II clathrate compounds $\text{Na}_{16}\text{Cs}_8\text{Si}_{136}$, $\text{Na}_{16}\text{Cs}_8\text{Ge}_{136}$, and $\text{Cs}_{24}\text{Sn}_{136}$. As expected, we find that as the host framework is

changed from Si to Ge to Sn, the heavier mass of the host atom causes the maximum vibrational energy to decrease, with the spectrum and all of its features compressed into a smaller energy region.

Of particular interest, for the possibility of obtaining a low thermal conductivity, are the localized (rattling) modes of the Na and Cs guests in the small (20 atom) and large (28 atom) cages. For $\text{Na}_{16}\text{Cs}_8\text{Si}_{136}$, we find that the localized modes associated with the Na motion in the small cages occur around 118 cm^{-1} to 121 cm^{-1} and that the localized modes associated with the Cs motion in the large cages occur at about 65 cm^{-1} to 67 cm^{-1} . Further, for $\text{Na}_{16}\text{Cs}_8\text{Ge}_{136}$, our predictions are that the rattler modes associated with Na motion in the small cages occur in the range 89 cm^{-1} to 94 cm^{-1} and that the Cs motion in the large cages leads to such modes at about 21 cm^{-1} to 23 cm^{-1} . The theoretical Raman active modes of these two materials have been presented in Ref. [40] and are in very good agreement with Raman scattering measurements.

Our results for the (so far) theoretical material $\text{Cs}_{24}\text{Sn}_{136}$ predict extremely low frequency guest rattler modes. Specifically, we find that the Cs motion in the 20-atom cages gives rise to localized modes around 25 cm^{-1} to 30 cm^{-1} . Further, Cs motion in the 28-atom cages produces guest rattler modes at frequencies from 5 cm^{-1} to 7 cm^{-1} . These very low frequencies arise because the Cs atom is very small in comparison with the 28 atom cage size (Sn_{28}). For the same reason, the resulting very weak potential is very anharmonic. Further, it should be kept in mind that the predicted Cs rattler frequencies were made within the harmonic approximation. Comparison of these predictions for $\text{Cs}_{24}\text{Sn}_{136}$ to experimental data is currently not possible. However, any future quantitative comparison between theory and experiment should correct these predictions taking into account the anharmonicity of the potential of the Cs in the large cages.

Finally, the rattler mode frequencies for Cs in the 28-atom cages in $\text{Na}_{16}\text{Cs}_8\text{Si}_{136}$, $\text{Na}_{16}\text{Cs}_8\text{Ge}_{136}$, and $\text{Cs}_{24}\text{Sn}_{136}$ have been discussed within a simple harmonic oscillator model for these modes. Combining the LDA-calculated Cs-to-host atom distances in these materials with this simple model has helped to explain the trend that there is a dramatic decrease in the rattler frequencies as the host material is changed from Si to Ge to Sn.

Acknowledgements We thank the NSF for grants (DMR-99-86706, DMR-96-32635) which supported this work. We thank Drs. G. Ramachandran and C. Kendziora and Profs. P. McMillan, R. Marzke, G. Nolas, and J. Gryko for helpful discussions.

References

- [1] G. S. Nolas, G. A. Slack, and S. B. Schujman, in: *Semiconductors and Semimetals*, Vol. 69, edited by T. M. Tritt (Academic Press, San Diego, 2000), p. 255, and references therein.
- [2] G. S. Nolas, J. W. Sharp, and H. J. Goldsmid, *Thermoelectrics: Basic Principles and New Materials Developments* (Springer-Verlag, Heidelberg, 2001).
- [3] N. P. Blake, S. Lattner, J. D. Bryan, G. D. Stucky, and H. Metiu, *J. Chem. Phys.* **115**, 8080 (2001).
- [4] V. L. Kuznetsov, L. A. Kuznetsova, A. E. Kaliazin, and D. M. Rowe, *J. Appl. Phys.* **87**, 7871 (2000).
- [5] J. D. Bryan, V. I. Srdanov, G. D. Stucky, and D. Schmidt, *Phys. Rev. B* **60**, 3064 (1999).
- [6] S. Yamanaka, E. Enishi, H. Fukukawa, and M. Yasukawa, *Inorg. Chem.* **39**, 56 (2000).
- [7] T. Yokoya, A. Fukushima, T. Kiss, K. Kobayashi, S. Shin, K. Moriguchi, A. Shintani, H. Fukuoka, and S. Yamanaka, *Phys. Rev. B* **64**, 172504 (2001).
- [8] F. M. Grosche, H. Q. Yuan, W. Carrillo-Cabrera, S. Paschen, C. Langhammer, F. Kromer, G. Sparr, M. Baenitz, Yu. Grin, and F. Steglich, *Phys. Rev. Lett.* **87**, 247003 (2001).
- [9] G. B. Adams, M. O'Keeffe, A. A. Demkov, O. F. Sankey, and Y. Huang, *Phys. Rev. B* **49**, 8048 (1994).
- [10] J. Gryko, P. F. McMillan, R. F. Marzke, G. K. Ramachandran, D. Patton, S. K. Deb, and O. F. Sankey, *Phys. Rev. B* **62**, R7707 (2000).
- [11] J. S. Tse and M. A. White, *J. Phys. Chem.* **92**, 5006 (1998).
- [12] G. S. Nolas, J. L. Cohn, G. A. Slack, and S. B. Schujman, *Appl. Phys. Lett.* **73**, 178 (1998).
- [13] J. L. Cohn, G. S. Nolas, V. Fessatidis, T. H. Metcalf, and G. A. Slack, *Phys. Rev. Lett.* **92**, 779 (1999).
- [14] G. S. Nolas, T. J. R. Weakley, J. L. Cohn, and R. Sharma, *Phys. Rev. B* **61**, 3845 (2000).
- [15] B. C. Chakoumakos, B. C. Sales, D. G. Mandrus, and G. S. Nolas, *J. Alloys Compd.* **296**, 80 (1999).
- [16] G. S. Nolas, B. C. Chakoumakos, B. Mahieu, G. J. Long, and T. J. R. Weakley, *Chem. Mater.* **12**, 1947 (2000).

- [17] B. C. Sales, B. C. Chakoumakos, R. Jin, J. R. Thompson, and D. Mandrus, *Phys. Rev. B* **63**, 245113 (2001).
- [18] S. Paschen, W. Carrillo-Cabrera, A. Bentien, V. H. Tran, M. Baenitz, Yu. Grin, and F. Steglich, *Phys. Rev. B* **64**, 214401 (2002).
- [19] G. S. Nolas and C. A. Kendziora, *Phys. Rev. B* **62**, 7157 (2000).
- [20] V. Keppens, B. C. Sales, D. Mandrus, B. C. Chakoumakos, and C. Laermans, *Philos. Mag. Lett.* **80**, 807 (2000).
- [21] V. Keppens, M. A. McGuire, A. Teklu, C. Laermans, B. C. Sales, D. Mandrus, and B. C. Chakoumakos *Physica B* **316–317**, 95–100 (2002).
- [22] J. Dong, O. F. Sankey, G. K. Ramachandran, and P. F. McMillan, *J. Appl. Phys.* **87**, 7726 (2000).
- [23] J. Dong, O. F. Sankey, and C. W. Myles, *Phys. Rev. Lett.* **86**, 2361 (2001).
- [24] C. W. Myles, J. J. Dong, and O. F. Sankey, *Phys. Rev. B* **64**, 165202 (2001).
- [25] C. W. Myles, J. J. Dong, O. F. Sankey, C. A. Kendziora, and G. S. Nolas, *Phys. Rev. B* **65**, 235208 (2002).
- [26] J. J. Dong and O. F. Sankey, *J. Phys.: Condens. Matter* **11**, 6129 (1999).
- [27] N. P. Blake, L. Mollnitz, G. Kresse, and H. Metiu, *J. Chem. Phys.* **111**, 3133 (1999).
- [28] G. B. Adams, M. O’Keeffe, A. A. Demkov, O. F. Sankey, and Y. Huang, *Phys. Rev. B* **49**, 8048 (1994).
- [29] J. J. Dong, O. F. Sankey, and G. Kern, *Phys. Rev. B* **60**, 950 (1999).
- [30] J. J. Dong, O. F. Sankey, G. K. Ramachandran, and P. F. McMillan, *J. Appl. Phys.* **87**, 7726 (2000).
- [31] J. Dong, O. F. Sankey and G. Kern, *Phys. Rev. B* **60**, 950 (1999).
- [32] J.S. Tse, Z. Li, and K. Uehara, *Europhys. Lett.* **56**, 261 (2001).
- [33] A. Moewes, E. Z. Kurmaev, J. S. Tse, M. Geshi, M. J. Ferguson, V. A. Trofimova, and Y. M. Yarmoshenko, *Phys. Rev. B* **65**, 153106 (2002).
- [34] M. Menon, E. Richter, and K. R. Subbaswamy, *Phys. Rev. B* **56**, 12290 (1997).
- [35] D. Kahn and J. P. Lu, *Phys. Rev. B* **56**, 13898 (1997).
- [36] Y. Guyot, B. Champagnon, E. Reny, C. Cros, M. Pouchard, P. Melinon, A. Perez, and J. Gregora, *Phys. Rev. B* **57**, R9475 (1998).
- [37] S. Bobev and S. C. Sevov, *J. Am. Chem. Soc.* **121**, 3795 (1999).
- [38] S. Bobev and S. C. Sevov, *J. Solid State Chem.* **153**, 92 (2000).
- [39] G. S. Nolas, D. G. Vanderveer, A. Wilkinson, and J. L. Cohn, *J. Appl. Phys.* **91**, 8970 (2002).
- [40] G. S. Nolas, C. A. Kendziora, J. Gryko, J. J. Dong, C. W. Myles, A. Poddar, and O. F. Sankey, *J. Appl. Phys.* **92**, 7225 (2002).
- [41] D. Vanderbilt, *Phys. Rev. B* **41**, 7892 (1990).
- K. Laasonen, R. Car, C. Lee, and D. Vanderbilt, *Phys. Rev. B* **43**, 6796 (1991).
- [42] G. Kresse and J. Hafner, *J. Phys.: Condens. Matter* **6**, 8245 (1994).
- G. Kresse and J. Hafner, *Phys. Rev. B* **48**, 13115 (1993).
- [43] This program was developed at the Institut für Theoretische Physik of the Technische Universität Wien. G. Kresse and J. Furthmuller, *Comput. Mater. Sci.* **6**, 15 (1996).
- [44] G. Kresse and J. Hafner, *Phys. Rev. B* **47**, 558 (1993).
- G. Kresse and J. J. Furthmuller, *Phys. Rev. B* **55**, 11169 (1996).
- [45] D. M. Ceperley and B. J. Alder, *Phys. Rev. Lett.* **45**, 566 (1980).
- [46] G. K. Ramachandran, P. F. McMillan, J. Diefenbacher, J. Gryko, J. Dong, and O. F. Sankey, *Phys. Rev. B* **60**, 12294 (1999).
- [47] C. Cros, M. Pouchard, and P. Hagenmuller, *J. Solid State Chem.* **2**, 570 (1970).
- [48] S. Bobev and S. C. Sevov, *J. Am. Chem. Soc.* **121**, 3795 (1999).
- [49] G. S. Nolas, J. L. Cohen, G. A. Slack, and S. B. Schujman, *Appl. Phys. Lett.* **73**, 178 (1998).
- [50] Y. Guyot, B. Champagnon, E. Reny, C. Cros, M. Pouchard, P. Melinon, A. Perez, and I. Gregora, *Phys. Rev. B* **57**, R9475 (1997).
- [51] N. W. Ashcroft and N. D. Mermin, *Solid State Physics* (Holt, Reinhart, and Winston, New York 1976), p. 500.
- [52] C. Kittel, *Introduction to Sol. Stat. Phys.*, 6th Edition (John Wiley & Sons, New York, 1986), p. 76.